Altered functional connectivity between cortical motor areas and the spinal cord in chronic stroke

Hanna Braaß[1,2*], Silke Wolf[1], Jan Feldheim[1], Ying Chu[2], Alexandra Tinnermann[2], Jürgen Finsterbusch[2], Christian Büchel[2], Christian Gerloff[1†] and Robert Schulz[1†]

[†]These authors contributed equally to this work.

[1] Department of Neurology, University Medical Center Hamburg-Eppendorf, 20246 Hamburg, Germany

[2] Department of Systems Neuroscience, University Medical Center Hamburg-Eppendorf, 20246 Hamburg, Germany

***Corresponding author:** Hanna Braaß, University Medical Center Hamburg-Eppendorf, Martinistraße 52, 20246 Hamburg, Germany, Email: h.braass@uke.de

Systems neuroscience research has significantly contributed to our current understanding of alterations in brain structure and function after ischemic stroke and their importance for recovery processes. Technical limitations have excluded the spinal cord from imaging-based research. Available data are restricted to few microstructural analyses. Functional connectivity data are absent. The present study sought to address this gap of knowledge and assess alterations in cortical and spinal cord activation and changes in corticospinal coupling in chronic stroke. Thirteen well-recovered patients underwent combined cortical and spinal functional MRI while performing a simple visually guided force generation task. Task-related activation was localized in ipsilesional primary motor cortex (M1), premotor ventral cortex (PMV), and supplementary motor area (SMA), as well as in the cervical spinal cord. Psycho-physiological interactions and linear modelling were used to infer functional connectivity between cortical motor regions and the cervical spinal cord and their associations with motor deficits. The main finding was that PMV and SMA showed topographically distinct alterations in their connectivity with the spinal cord. Specifically, for SMA, we found a reduced coupling with voxels localised in the ipsilateral ventral spinal cord. For PMV, an enhanced coupling was detected with ventral, and intermediate central spinal zones. Lower SMA- and higher PMV-related spinal cord couplings located in similar areas were directly correlated with residual deficits. Collectively, this work provides first-in-human functional insights into stroke-related alterations in the functional connectivity between cortical motor areas and the spinal cord with patterns of directionality and topography suggesting that different premotor areas and spinal neuronal assemblies might be differentially prone to and involved in coupling changes. It adds a novel, promising approach to better understand stroke recovery in general, and to develop innovative models to comprehend groundbreaking treatment strategies with spinal cord stimulation.

Introduction

Imaging-based systems neuroscience research has significantly contributed to our current understanding of alterations in brain structure and function after ischemic stroke and how they relate to deficits and recovery processes. Apart from cognitive and language functions, deficits in the motor domain, particularly affecting the upper limb, are important sequelae after stroke impeding private and professional rehabilitation[1]. Structural[2] and functional imaging[3,4] have built a robust body of evidence showing how acute stroke lesions affect brain activation and multi-site communication patterns as well as the structural integrity of the human motor network and its key areas and interconnecting pathways comprising the primary motor cortices (M1), frontal secondary motor areas including the ventral premotor cortex (PMV), and the supplementary motor area (SMA), subcortical brain regions, and the cerebellum. The corticospinal tract (CST), as the main outflow system of the motor network, has been mostly addressed structurally at various cerebral levels via lesion load[5], fibre count[6,7] and diffusion-imaging based analyses of white matter microstructure[2,8]. Recently, advanced structural MRI extended the field of view towards the brain stem and the cervical spinal cord regarding structural CST alterations[9]. Collectively, such CST data were convergingly reported to be critically linked to stroke recovery. Notably, studies showed that not only CST fibres originating from M1, but also secondary CST originating from non-primary motor areas, such as PMV and SMA[10] show structure-outcome associations[8,11–15]. It has been repeatedly discussed that such CST might mediate

corticospinal neurotransmission while bypassing lesioned CST components[16–20]. For instance, higher SMA activity in EEG[21] and stronger structure-outcome associations for M1-PMV pathways[17,22] were found particularly in patients with more CST damage. It has been speculated that these alternate CST trajectories might act on lower motor neurons directly, or much more likely, indirectly via modulation of spinal interneuronal assemblies and circuits[23,24]. After earlier reports on spinal cord and circuit dysfunctions after stroke[25], and the first report of successful epidural cervical spinal cord stimulation for improvements of chronic post-stroke upper-limb paresis just recently[26], the interest in the spinal cord after cortical stroke experienced a remarkable renaissance[27–29]. Animal data had already suggested that the spinal cord might be involved in recovery processes after cortical motor stroke[30–33]. However, functional data on spinal cord activations and functional connectivity with cortical motor networks are not available so far. However, such analyses would of great value, not only to better understand stroke recovery in general, but also to shed light on such groundbreaking innovative treatments protocols with spinal cord stimulation, in particular.

Advancements in functional MRI (fMRI) of the spinal cord[34,35], and simultaneous cortical and spinal cord fMRI[36,37] opened a new window to investigate functional corticospinal networks in humans with high spatial resolution[38]. In the motor domain, studies have just started to explore corticospinal functional connectivity during finger or hand movements in healthy participants[35,39–41]. In our previous study we were able to link ventral spinal activation during simple hand movements not only to M1 activation, but also PMV activation[41]. This added first fMRI data to sparse transcranial magnetic stimulation data[42–44] which had suggested that human premotor areas might be functionally connected to the lower cervical spinal cord, likely interneurons, and contribute to distal upper limb functions in humans.

The present study was designed to start out exploring, for the first time in human stroke survivors, alterations in cortical and spinal cord activation and changes in corticospinal coupling during a simple visually guided force generation task. Task-related activation was localized in ipsilesional M1, PMV, and SMA, and the cervical spinal cord. Task-related spinal cord activation and psycho-physiological interactions (PPI) were inferred to assess functional connectivity between cortical motor regions and the cervical spinal cord, linear modelling was used to address their associations with motor deficits.

Materials and methods

Subjects

Fourteen chronic stroke patients participated in the study. Inclusion criteria were first ever ischemic stroke ≥ 6 months leading to a persistent motor deficit involving the hand function and age between 18 and 80 years. Exclusion criteria were preexisting clinically silent brain lesions > 1cm^3 on MRI, pre-existing motor deficits, contraindications against MRI, psychiatric disease, and active drug abuse. One patient had to be excluded from final analysis because the MRI experiment was terminated prematurely. The resulting 13 patients were matched with 13 age-matched healthy controls without any neurological damage unrelated to healthy aging. All participants were right-handed according to the Edinburgh handedness inventory[45] and provided informed consent, following the Declaration of Helsinki. The study was approved by the local ethics committee of the Medical Association of Hamburg (PV6026). All subjects received monetary compensation.

Motor Task

A simple motor task was used comprising repetitive whole-hand grips in a block design as previously introduced in detail[41]. In three active conditions, stroke patients performed repetitive visually guided, almost isometric whole-hand grips with their affected hand with three varying predefined force levels (low, medium, and high corresponding to 30%, 50%, and 70% of the maximum output measurement) using an MRI compatible grip force response device (Grip Force Bimanual, Current Design, Inc, Philadelphia, PA). Healthy controls performed the task with the right or left hand corresponding to the affected side of the matched patients (“pseudo-side”). In the active condition, a white cross presented on a screen blinked at 0.8Hz which indicated the frequency of hand grips. Details of the time course of each block have been reported previously[41].

MRI data acquisition

A 3T Prisma MRI scanner (Siemens Healthineers, Erlangen, Germany) and a 64-channel combined head-neck coil were used to acquire cerebral and spinal imaging data. The MRI protocol was identical to the previously described MRI protocol[41]. The imaging modalities included high-resolution T1, T2*-weighted, and task-related fMRI images with the iso-center approximately centered to vertebral level C2/C3. For the T1-weighted sequence, a 3-dimensional magnetization-prepared rapid gradient echo (3D-MPRAGE) sequence was used, which covered the head, the cervical spine and the upper part of the thoracic spine with the following parameters: repetition time (TR) = 2300ms, echo time (TE) = 3.4ms, flip angle 9°, 236 coronal and 320 axial slices, voxel size: 1.0 x 1.0 x 1.0mm³. The T2*-weighted image (MEDIC sequence) covered the identical part of the cervical spine as the functional spinal slices, centered on vertebra C6, with the following parameters: TR = 307ms, TE = 21ms, flip angle 20°, eight axial slices, voxel size: 0.5 x 0.5 x 5.0mm³. For task-related fMRI, a combined corticospinal protocol based on echo-planar imaging (EPI) was used to record BOLD responses in the brain and spinal cord[37,38] covering 32 slices, divided into two sub-volumes (**Supplementary Figure S1**). These two sub-volumes had different geometry, timing parameters, and shim settings[36]. The shim settings were determined using a field map acquisition and a dedicated shim algorithm[36]. The upper volume included 24 axial slices (voxel-size: 2.0 x 2.0 x 2.0mm³, 1mm gap between slices) in the brain. The lower sub-volume consisted of 8 axial slices (voxel-size: 1.0 x 1.0 x 5.0mm³, no gap between slices), centered at the vertebral body of C6 and covered the vertebral bodies of C5, C6, and C7. The whole sequence was measured with the following parameters: TR = 2231ms, TE = 30ms/31ms (brain/spinal cord), flip angle = 75°. Additionally,

one whole-brain EPI volume was measured with the following parameters: TR = 2385ms, TE = 30ms, flip angle 75°, 36 axial slices, voxel size: 2.0 x 2.0 x 2.0mm³, 1mm gap between the slices. During the fMRI sessions, pulse, respiration, and the trigger signal were recorded (sampling rate = 400Hz) using the Physlog-function (Ideacmdtool) and respiratory and pulse measurement devices provided by Siemens Healthineers, Erlangen, Germany.

Behavioral data

The individual maximum whole hand grip force of both hands was measured with a JAMAR Hand Dynamometer (built by Patterson Medical, Warrenville, USA). Further standardized tests included the National Institutes of Health Stroke Scale (NIHSS), the Fugl Meyer Assessment of the upper extremity (UEFM), the modified Rankin Scale (MRS), and the Nine-hole peg test (NHP). Healthy controls underwent grip force measurement and NHP testing. Relative NHP values were calculated by dividing the values of the affected and unaffected side, or pseudo-sides, respectively.

Image preprocessing

In line with our previous study[41], brain and spinal cord images were pre-processed separately. The brain fMRI images were pre-processed using the Oxford Center for fMRI of the Brain's (FMRIB) Software Library (FSL) v. 6.0.4[46]. Un-flipped data were used for the readout of the individual BOLD parameters. For the second-level analysis, all T1-weighted and EPI brain images with right-sided stroke lesions were flipped to the left hemisphere. This hemispheric flip was also performed in the matched controls. The whole-brain EPI image of each subject was linearly co-registered to the individual high-resolution T1-weighted brain images, and the individual T1-weighted image was linearly co-registered with the MNI152 T1-2mm image from the FSL library. The transformation matrices were concatenated for further preprocessing steps. The first five dummy volumes of the task-related fMRI images were discarded, and the averaged fMRI image was registered to the whole brain EPI image. The concatenated transformation matrices were then used for registration to the MNI152-T1-2mm image. The fMRI images were further pre-processed with motion correction using MCFLIRT[47], and the images from both sessions were concatenated into one time series at the subject level.

The spinal fMRI images were pre-processed using the Spinal Cord Toolbox, v. 5.2[48], and FSL v. 6.0.4[46]. For the second level analysis, all T2*-weighted and spinal EPI images of patients with right-sided stroke lesions and their matched controls were flipped to the right side of the spinal cord and the un-flipped data were used for readout of individual BOLD parameters. The first step was that the spinal fMRI images were cropped with the spinal cord at the center of the image. Motion correction was performed using two phases of movement correction: MCFLIRT[47] was used for the first phase with spline interpolation and a normalized correlation cost function. The images across the two runs were realigned to the first image of the first run with a three-dimensional rigid-body realignment. To correct slice-independent motion, the second phase of motion correction was performed with two-dimensional rigid realignment independently for each axial slice[35,49]. The images from both sessions were concatenated into one time series at the subject level.

The spatial normalization from native to MNI standard space was performed using tools from the open-source Spinal Cord Toolbox[35,48]: The structural T2*-weighted images were normalized to the PAM50_T2s-template (resolution = 0.5 x 0.5 x 0.5mm³)[35,50]. After motion correction, the mean functional image was segmented to identify the spinal cord. The resulting binary spinal cord mask and the reversed deformation fields of the structural normalization were used to register the PAM50_T2-template on the mean functional image. The inverted resulting deformation field was then used for image normalization to PAM50-space. All normalized images were visually inspected for quality control at each step.

Physiological noise modelling

Cardiac and respiratory cycles are significant noise sources in spinal cord fMRI and can confound signal detection[35]. The SPM (SPM12) based PhysIO Toolbox version 8.1.0[51], ran in MATLAB version R2018a, was used to calculate the noise regressors. This toolbox uses a model-based physiological noise correction, which uses retrospective image correction (RETROICOR) of physiological motion effects[52], heart rate variability[53], and respiratory volume per time[54]. Based on the physiological signals, 18 noise regressors were generated. A cerebrospinal fluid (CSF) regressor was also generated from the CSF signal surrounding the spinal cord using a subject-specific CSF mask generated from the PAM50_csf-template[35,50].

First level analyses

Two different first- and second-level analyses were performed. The analyses of the cerebral and spinal images were conducted separately. For both analyses, the same explanatory variables (EVs) were used in the design matrices of the general linear models (GLM).

First first-level analysis: For each volume (TR) the averaged maximum force produced was calculated and used as EV in the design matrix and, from now on, referred to as activation during the task. In the second first-level analysis, the low, medium, and high force levels were used as EVs. In both analyses, the temporally jittered instruction period[41] was separately modelled as an additional EV but not further analysed in the group analysis[55]. The brain and spinal cord data were analysed separately.

Brain images: the motion-corrected functional images were spatially smoothed with a Gaussian kernel of 5mm full-width half maximum (FWHM) and high-pass filtered (90s) using the fMRI Expert Analysis TOOL (FEAT v6.00)[56,57]. Statistical maps of the pre-processed time series were generated using FMRIB's improved Linear Model (FILM) with pre-whitening[35,57]. The design matrices included the hemodynamic response function (gamma convolution, phase 0s, standard deviation 3s, mean lag 6s) convolved task vectors as EVs. Motion parameters, and motion outliers, determined using

fsl_motion_outliers were entered as covariates to remove movement-related variance. The voxels of peak activation in the subject-specific activation maps for the task related activation EV were localised in ipsilesional M1, PMV and SMA, according to the Harvard-Oxford atlas (SMA and precentral gyrus, M1) and the HMAT template (Human motor area template)[58] (PMV) for correct localisation. For the second-level analyses, spatial normalization of the statistical images from the subject-level analyses to the MNI template was performed.

Spinal images: the motion-corrected functional images were spatially smoothed with a Gaussian kernel of 2 x 2 x 5mm FHWM, and the spinal cord was extracted from the data using a spinal cord mask, which was created from the PAM50_cord_template and spatial transformed in the subject-specific space. The data were further analysed with FEAT and high pass filtered (90s). The statistical maps of the pre-processed time series were generated using FILM with pre-whitening. The design matrices included the hemodynamic response function (gamma convolution, phase 0s, standard deviation 3s, mean lag 6s) convolved task vectors as EVs, the physiological noise regressors, the CSF time series, the motion parameters and motion outliers as covariates of no interest. The voxels of peak activation in the subject-specific activation maps for the task related activation were localised in the ipsilesional (ipsilateral to the moving hand) spinal cord. For the second-level group analysis, spatial normalization of the statistical images from the subject-level analyses to the PAM50-template was performed.

Second level analyses

Each group's average activation maps were generated with the demeaned individual maximum grip force of the measured hand, side, and age as additional covariates using FMRIB's Local Analysis of Mixed-effects (FLAME) stages 1 and 2[56,59]. The group average activation maps were thresholded using a *Z-Score* > *2.4* with a cluster significance threshold of $P < 0.05$ to correct for multiple comparisons using GRF (Gaussian Random Field) theory[39]. Group comparison was calculated for the task-activation with maximum grip force as an additional covariate. The activation maps for the contrasts [stroke > control] and [control > stroke] were thresholded using a *Z-Score* > *2.0* with a cluster significance threshold of $P < 0.05$.

Psycho-physiological interaction

To assess the functional connectivity between the brain and the spinal cord psycho-physiological interaction (PPI) models were implemented with seed regions in ipsilesional M1, PMV, and SMA. The time course was extracted from spherical regions of interest (ROI) with a radius of 2mm around the peak voxel for each region in each subject. PPI models were calculated in the spinal cord with the extracted time course of each brain region. The models contained the same task regressors as in the model of the whole task, the mean centred time course, and the PPI interaction term with the task activation. In addition, the models contained all regression terms for movement and physiological noise as in the original GLM. Group comparison was calculated for each region with individual maximum grip force as additional confound parameter using FLAME 1 and 2, the Z-maps were thresholded using a *Z-Score* > *2.0* with a cluster significance threshold of $P < 0.05$.

In two additional analyses in the stroke patients, demeaned relative NHP and demeaned UEFM were included to analyse the relationship between motor impairment after stroke and functional connectivity, corrected for maximum grip force, age and side. The Z-maps were thresholded using a *Z-Score* > *2.4* with a cluster significance threshold of $P < 0.05$.

The estimated coupling strength was extracted from different spinal voxels (the specific coordinates are given in the figures showing the PPI results).

Further statistical analyses

The statistical package R 4.3.1[60] was used for statistical analysis. Linear models were used to analyse age, NHP ratio and maximum grip force for group specific differences, with "side" as additional confound of no interest. Two-sided t-tests were used to compare the exerted forces between the groups.

Results

Demographic, clinical and task data

Thirteen chronic stroke patients (twelve males and one female, all right-handed, aged 62.6 ± 9.7 years, mean ± SD) and 13 healthy controls (eight males and five females, all right-handed, aged 64.5 ± 11.9 years) were included in this work. Patients and controls were matched for the measured/affected hand. Clinical characteristics are given in **Table 1**. There were no significant group differences for age ($P = 0.65$) or maximum grip force ($P = 0.75$). The NHP ratio was numerically higher in the stroke patients ($P = 0.056$). A topographic map of the distribution of stroke lesions is shown in **Figure 1**. During the motor task, the exerted target forces for stroke patients were 42.0 ± 8.5%, 61.0 ± 8.4% and 76.7 ± 10.97% for low, medium, and high levels, respectively. For controls, they were 43.7 ± 12.2%, 60.2 ± 8.0%, and 77.9 ± 6.5%, respectively, with no group differences.

Spinal cord and cortical activation during force generation

Force generation across all three force levels led to a significant activation on group level primarily in the ipsilesional (= ipsilateral to the measured/affected hand) spinal cord between the lower parts of the C6 and C7 vertebral level, corresponding to the C7 and C8 spinal segments in both groups (**Figure 2, A, B**). The stroke patients exhibited a higher activity than controls, localized in the middle of the spinal cord cross-section between vertebra C6 and C7 (**Figure 2, C**). The cluster characteristics are listed in **Supplementary Table T1**. In the stroke patients, increasing force levels led to an increase in the spatial extent of BOLD responses from a focal activation at the C7 vertebral level towards more distributed spinal activations between C5 and C7 (**Supplementary Figure S2, A)**. In the control group, a similar increase was observed from a focal activation at the C5 vertebral level during low forces towards more distributed spinal activations between C5 and C7 (**Supplementary Figure S2, B**).

Table 1 Characteristics of patients and healthy controls

ID	Age range	Sex	Lesioned hemisphere	Lesion volume [ml]	Time since stroke [months]	Maximum Grip force [Kg]	UEFM	NHP ratio [aff/unaff]	MRS	NIHSS
S1	35-40	m	Left	0.1	43	49.7	65	0.95	1	1
S2	61-65	m	Left	1.2	118	38.0	59	1.06	1	0
S3	61-65	m	Left	0.4	12	30.0	60	0.91	1	0
S4	71-75	m	Right	36.8	159	28.7	45	1.41	2	2
S5	56-60	m	Left	0.3	9	39.3	64	0.96	1	0
S6	66-70	m	Left	0.3	55	40.7	50	1.62	2	1
S7	61-65	m	Left	0.1	56	48	60	1.20	1	1
S8	66-70	m	Right	34.4	7	50.7	59	1.07	1	1
S9	71-75	w	Right	3.4	6	25.3	59	1.21	1	0
S10	56-60	m	Left	31.6	53	48.7	53	1.09	2	3
S11	66-70	m	Right	64.9	16	39.0	58	0.95	1	0
S12	46-50	m	Left	4.3	65	54.7	64	0.96	1	0
S13	61-65	m	Left	0.7	20	40.7	60	0.98	1	0
Patients	62.6 (9.7)	1 W / 12 M	9 Left / 4 Right	13.74 (21.08)	47.62 (46.32)	41 (9)	58.15 (5.73)	1.11 (0.21)	1.23 (0.44)	0.69 (0.95)
Controls	64.5 (11.9)	5 W / 8 M	9 Left / 4 Right[a]			40 (10)[b]		0.98 (0.13)[b]		

Characteristics of all patients individually and averaged per group for patients and controls. Mean values and standard deviation in brackets are given. Examination date of MRI imaging in months after stroke. UEFM = Upper Extremity Fugl Meyer Assessment. MRS = modified Rankin Scale. [a] healthy controls: examined side, left = right hand / left hemisphere, right = left hand / right hemisphere. [b] healthy controls: aff = examined hand.

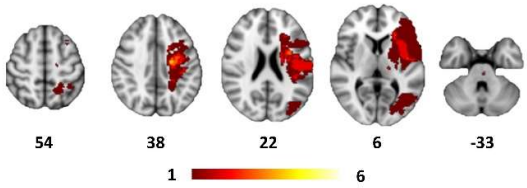

Figure 1 | Topography of stroke lesions
All masks of stroke lesions are projected on the left hemisphere, overlaying a T1-weighted template in MNI space (z-coordinates below each slice). The colour intensity indicates the number of subjects of whom lesion voxels lay within the coloured region.

Cortical activity on group level was detected in both groups across force levels primarily in the ipsilesional primary sensorimotor cortex comprising M1 and the primary sensory cortex S1, in bilateral SMA, bilateral dorsal premotor cortex, bilateral PMV and a widespread activation in posterior parietal cortices along the intraparietal sulcus (**Figure 2, D, E**). Group comparisons revealed higher activity in the M1, SMA and bilateral intraparietal sulcus in the stroke group (**Figure 2, F**). The results of the force-level specific analyses are shown in **Supplementary Figure S3**. Cluster characteristics of the task activation are listed in **Supplementary Table T2**.

Corticospinal connectivity during force generation

Psycho-physiological interactions (PPI) were computed to investigate task-specific functional corticospinal coupling. Compared to controls, stroke patients exhibited a significantly reduced connectivity between SMA and ventral spinal voxels comprising ventral horn areas and surrounding white matter at ipsilesional and contralesional lower C6 vertebral level (**Figure 3, A, B**). In contrast, connectivity was found to be enhanced between PMV and an intermediate spinal zone at C5 and ventral areas at the upper C6 vertebral levels. (**Figure 3, C, D**). For M1-spinal cord connectivity, only a small cluster in the upper part of vertebral level C6 was detected in which stroke patients showed a reduced task-related coupling (**Figure 3, E, F**). Additional cluster results are listed in **Supplementary Table T4**.

Corticospinal coupling and motor impairment

Coupling-behaviour correlations revealed that patients which exhibited lower SMA- and higher PMV-spinal cord coupling showed more severe motor deficits as assessed by means of NHP ratio and UEFM (**Figure 4, A-D**). Specifically, for SMA, we detected a ventral location in which reduced, i.e., negative connectivity was correlated with more severe deficits. Importantly, the location of this cluster was congruent with the location in which we found the loss of corticospinal connectivity for SMA (**Figure 3, A**). For PMV, we detected one cluster in the ventral spinal cord at z = -170 (MNI) in which an increase in connectivity (see **Figure 3, D**) was correlated with lower UEFM scores (**Figure 4, C, D**). For fine motor skills, assessed via NHP ratio, one additional cluster was found in the intermediate zone below the spinal level in which we detected an increased corticospinal connectivity after stroke (**Figure 4, A, B**).

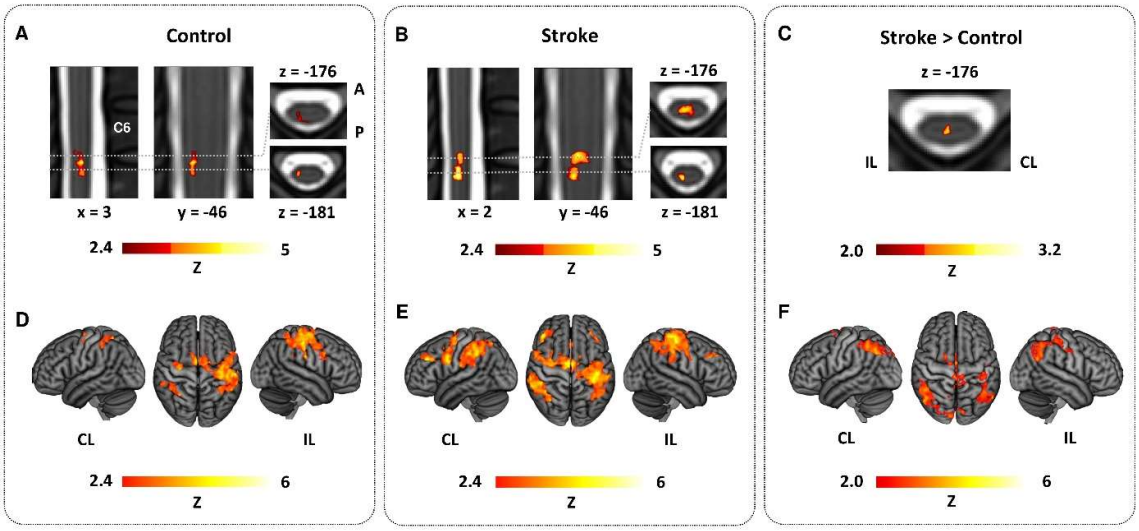

Figure 2 | Topography of spinal cord and cortical brain activation during force generation
(A), **(B):** Estimated group mean spinal activation during the task, maximum grip force, side and age were included as additional confound parameters for the control group (**A**) and stroke group (**B**); **(C)** spinal BOLD response with the contrast [stroke > control], controlled for maximum grip force; (**D**), **(E):** Estimated group mean cerebral activation during the task, max. grip force, side and age were included as additional confound parameter for the control group (**D**) and stroke group (**E**); **(F)** [stroke > control] contrast, controlled for max. grip force. Z-maps were thresholded by $Z > 2.4$ (group mean) and $Z > 2.0$ (group comparison), cluster significance threshold of $P < 0.05$; Spinal cord activations are overlaid on the PAM50_t2-template. Cerebral activations are rendered on a T1 template in MNI space. IL=ipsilesional, CL=contralesional, A=anterior, P=posterior

Finally, for M1, only a relatively small cluster localized in the ventral spinal cord of C5 vertebral level (**Figure 4, E)** showed a correlation between higher connectivity and more motor impairment. However, this cluster did not show stroke-related alterations in corticospinal connectivity with M1, which limits the value of this finding. Additional cluster results are listed in **Supplementary Table T5**.

Discussion

The main finding of the present study was that chronic stroke patients show alterations in activation and connectivity between cortical motor areas and the spinal cord while performing a simple force generation task with the affected hand. Compared to healthy controls, patients were found to activate central spinal regions, potentially paralleling intermediate interneuronal zones, between vertebral levels C6 and C7, more strongly. In terms of connectivity, noticeable and topographically distinct, and clinically relevant alterations were particularly revealed for corticospinal coupling affecting the ventral premotor cortex (PMV) and the supplementary motor area (SMA) with opposite directions: For SMA, we found a reduced coupling with voxels localizing in the ventral spinal cord at lower C6 vertebral levels. For PMV, an enhanced coupling was detected with ventral regions at upper C6 vertebral levels and intermediate central spinal zones at C5 level. Finally, lower SMA- and higher PMV-related spinal cord coupling located in similar areas, most likely contributing to the ipsilateral ventral areas, was directly correlated with residual deficits.

These data provide first-in-human functional insights into possible corticospinal network alterations after stroke and thereby add a novel, promising functional perspective to the emerging field of spinal cord analyses and stimulation in stroke recovery research.

The present work is based on previous animal and human imaging and electrophysiology data arguing that the spinal cord may be considered an important, however largely neglected, factor to modulate recovery after cortical stroke. For instance, previous animal work has evidenced an upregulation of spinal structural plasticity, neurotrophins, and cytokines[61,62]. Recent transcriptome analyses found gene upregulations related to neurite outgrowth in stroke-denervated spinal gray matter, particularly in its intermediate laminae[30]. One study reported spinal axonal sprouting and microglial activation to support presynaptic site formation[31], potentially occurring in central spinal regions in which axonal outgrowth has been consistently documented in stroke animal models[32,63]. Interestingly, at group level, we also found an increase in spinal cord activation in similar central voxels. Furthermore, stronger PMV coupling in two additional central clusters was correlated with greater deficits. Speculative in nature, such areas might correspond to intermediate zones such as lamina X or, even more specifically, interneurons from V0 families, which were reported to contribute to complex corticospinal circuits connecting motor, sensory cortical influences with spinal neuronal assemblies[23,24]. Animal studies suggest that these assemblies are involved, for example, in left-right coordination[64] or aberrant excitation during progression of amyotrophic lateral sclerosis[65]. As a second topographically interesting finding, alterations in corticospinal coupling were detected for areas localizing towards the ipsilateral ventral spinal cord.

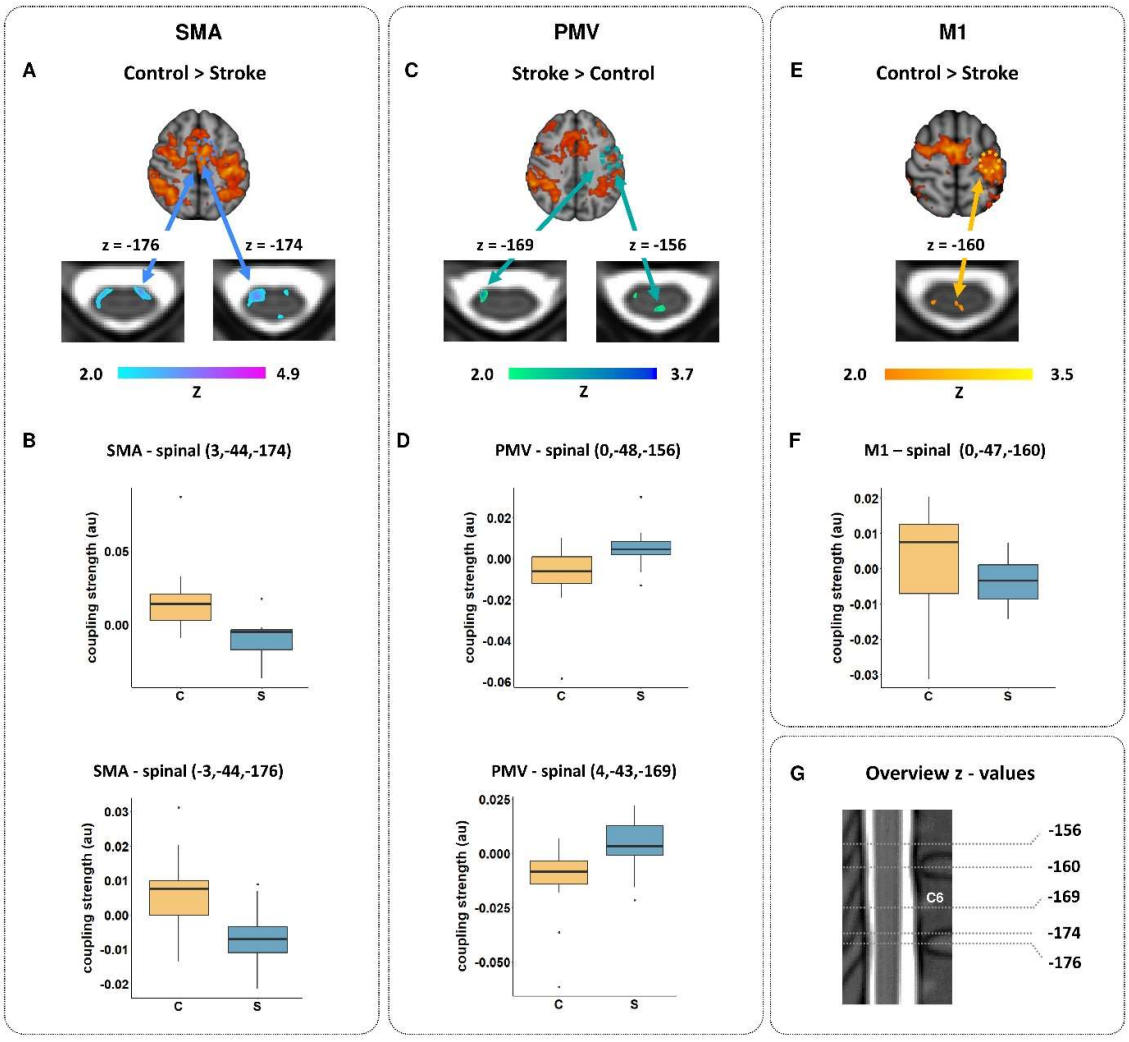

Figure 3 | Alterations in corticospinal coupling during force generation
PPI analysis between ipsilesional SMA (blue, **A/B**), PMV (green, **C/D**), and M1 (yellow, **E/F**) and the spinal cord. Z-maps are thresholded by *Z > 2.0*, cluster significance threshold of *P < 0.05.* Topography of spinal voxels exhibiting significant group differences in coupling are depicted on axial spinal slices with z-values given in MNI space (**A-C**). Spinal cord activations are overlaid on the PAM50_t2-template. Cerebral and spinal images are in radiological orientation. **G** Overview of the slices displayed along the z-axis. For illustration purposes, cerebral activation maps are taken from **Figure 2, E**. Coupling strengths in spinal cluster-voxels (cluster peak- and exemplary voxels) are depicted by box plots for both groups including MNI coordinates of the voxels (**B, D, F**). C=control, S=stroke.

Particularly for SMA, the overlap between voxels exhibiting a reduced connectivity and voxels exhibiting a correlation with behaviour was notable. Ipsilateral ventral horn areas would be in line with the location of lower motor neurons or V1 interneuron populations comprising multiple cell types, including Renshaw cells and Ia inhibitory interneurons[66–68]. It remains elusive if any, or which, neuronal component might be particularly related to the associations found in the present fMRI datasets. At least from a very simplified clinical view, the patients included in this analysis did not show hand spasticity in hand/finger flexion and extension. Larger samples with varying degrees of spasticity could allow for regression modelling of this valuable covariate. Combined approaches with electrophysiology, such as single-fibre electromyography, could add to the regression of trans-synaptic degeneration of spinal motor neurons after stroke[69].

It was an unexpected finding that couplings between M1 and the spinal cord were sparse in terms of spatial distribution and congruency between connectivity and coupling-outcome relationships. Considering that M1 contributes to the majority of CST fibres[10], and the structural state of its trajectories has been repeatedly shown to be an important determinant of recovery after stroke[2,8,12], it was comprehensible to hypothesize that M1-related corticospinal functional coupling should be a relevant finding also in our analyses. However, the present analyses yielded more convincing data that PMV and SMA were linked to the spinal cord and motor deficits after chronic stroke. In fact, similar findings were also reported by some structural analyses in which CST originating from premotor areas explained more variance than M1-related CST in clinical scores, or significantly enhanced CST-outcome correlations[8,11,13,14,70,71].

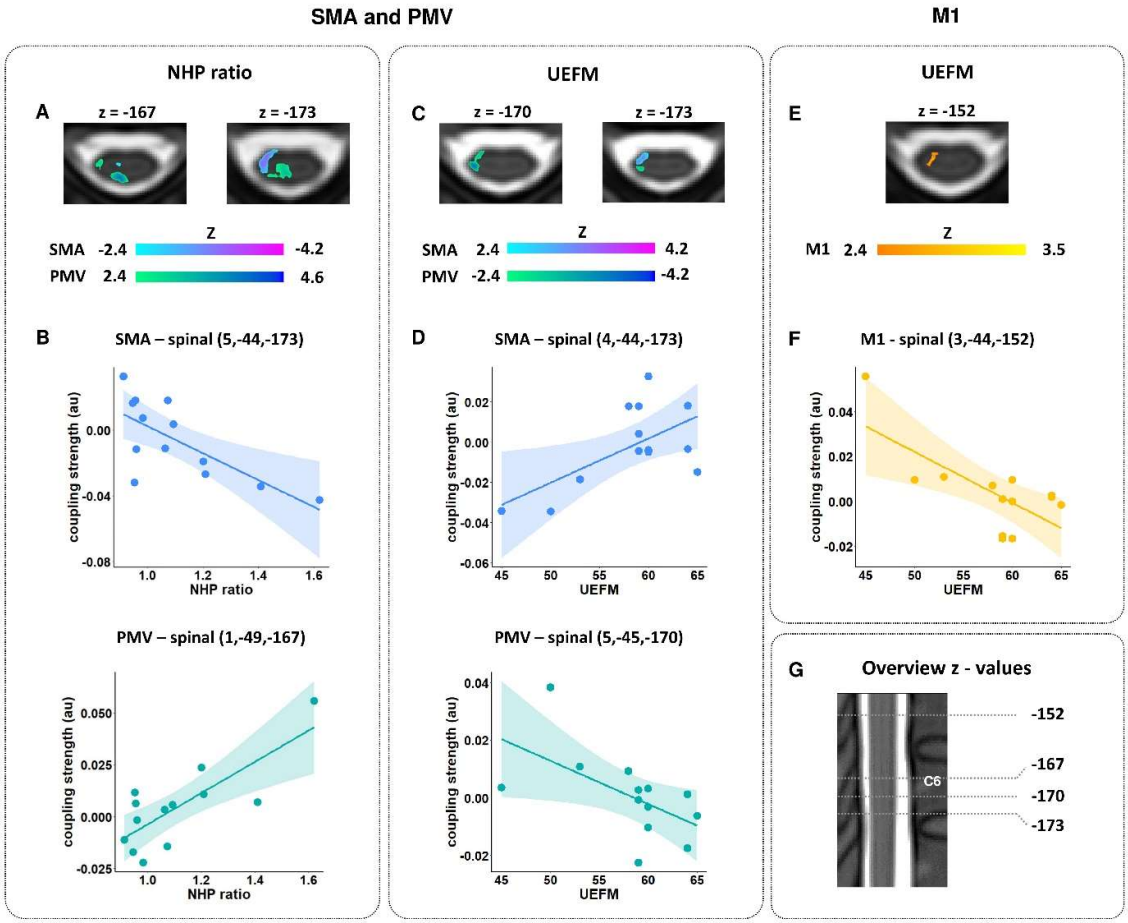

Figure 4 | Associations between corticospinal coupling during force generation and motor impairment
Topographic maps and linear regression plots for correlations between PPI-derived PMV- (green) and SMA- (blue) related corticospinal connectivity and the clinical parameters NHP (**A, B**) and UEFM (**C, D**), respectively. An M1-related map and regression plot is given in **E, F**. **G** Overview of the slices displayed along the z-axis. Z-maps thresholded by $|Z| > 2.4$, cluster significance threshold of $P < 0.05$, grip force, side and age were included as additional confound parameters, spinal cord activations are overlaid on the PAM50_t2-template. Spinal images are in radiological orientation.

Limited data also arises from electrophysiological experiments in chronic stroke patients in which the excitability of the CST was positively correlated with the structural integrity along the length of CST emerging from premotor cortices, but not M1[72].

Recent human data have convergingly evidenced, potentially against previous assumptions derived from non-human primates[73–76], that PMV and SMA might be structurally[77] and functionally connected[42,78] not only with upper segments of the spinal cord, but also with lower cervical spinal cord contributing to distal upper limb functions. These connections are likely to be maintained by poly-synaptic connections along spinal interneural routes including the propriospinal system[79]. The present data build on this knowledge. They confirm that premotor areas might be functionally linked to lower cervical spinal cord and add that the connectivity undergoes changes after stroke which are linked to clinical aspects. Unfortunately, we can only speculate about the meaning of the directions of alterations and linear associations. For instance, the negative coupling between SMA and the ventral spinal cord could be interpreted as an inhibitory process during the execution of the task [80]. How this coupling might mechanistically explain the level of impairments remains open for discussion and controversy[3,4,21,81].

Functional analyses of corticospinal coupling and spinal cord activation might help to better understand stroke recovery in general. However, this approach might be particularly promising to comprehend effects of spinal cord stimulation after stroke, especially in light of recent breakthrough results demonstrating improvements in arm and hand paresis in two chronic stroke patients[26]. It has been speculated that spinal cord stimulation might act via the recruitment of primary afferents, which provide excitatory input to motoneurons, and interneurons directly connected to such afferents. Thereby, spinal stimulation might increase the responsiveness to residual cortical inputs, e.g., from preserved primary and non-primary CST, or alternate descending pathways including the reticulospinal tract[2,9,82,83]. Enabling researchers to assess

changes in corticospinal activation and connectivity with sufficient spatial resolution, as illustrated in our study, corticospinal fMRI could contribute to disentangling mechanisms such as increases in motoneuron excitability, postsynaptic inhibition, or sensory gating, which have been discussed as potential mechanisms for spinal cord stimulation[27].

There are several important limitations to note. First, the small sample size must be considered when interpreting the results. Despite technical advances, spinal cord imaging remains a time-consuming challenge, particularly when it comes to older participants. Inclusion criteria were rather strict, more severely impaired patients could not perform the task properly and could therefore not participate in this study. Future studies on larger sample sizes are needed to verify the present results and may help to generalize them to the broader population. Potentially, a simpler motor task together with further improvements in shim algorithms and MRI sequences for better Signal-to-Noise-Ratio (SNR) and shorter acquisition times might aid to improve recruitment and data quality. Second, the design of this study was cross-sectional. A longitudinal approach could provide further insights into the temporal dynamics of stroke-related changes in corticospinal coupling and activation. The extent to which the observed group differences result from progressive up- or downregulation over time, which would be a compelling argument, remains to be investigated. Third, the limitations also affect imaging artifacts related to movement and physiological signals. We sought to minimize them by adapting our analysis pipeline according to established protocols for spinal fMRI artifact minimization. The cerebral and spinal fields of view were rather small due to technical restrictions. Congruent with our previous work in younger, healthy participants[41] and given a broad evidence suggesting that M1, PMV and SMA are key areas which undergo stroke-related changes in brain structure and function[2–4], we focused our analyses on these cortical areas. Subcortical nodes of the human motor network, such as basal ganglia, the cerebellum and the brainstem comprising descending tracts such as the reticulospinal tract, could not be included as seed areas in this work. Finally, the spinal resolution was limited which complicates the inference of precise topographical interpretations regarding spinal neuronal assemblies. Future studies are needed to address these important aspects, the integration of other seed areas could broaden the picture of functional connectivity changes between cortical, subcortical and the spinal cord after stroke.

Conclusion

Collectively, this work provides first-in-human functional insights into stroke-related alterations in the functional connectivity between cortical motor areas and the spinal cord. The analysis of directionality and topography of the results suggests that different premotor areas and spinal neuronal assemblies might be differentially prone to and involved in coupling changes. This study adds a novel, promising approach to better understand stroke recovery in general, and to develop innovative models to comprehend groundbreaking treatment strategies with spinal cord stimulation.

Data availability

All data needed to evaluate the conclusions in the paper are present in the paper and/or the Supplementary Materials. Processed brain and spinal cord activation data and demographic data to reproduce the findings are available from the corresponding author upon reasonable request.

Funding

This work was funded by the Deutsche Forschungsgemeinschaft (DFG, German Research Foundation) SFB 936 - 178316478 - C1 (CG) & A6 (CB) and Exzellenzstipendium from the Else Kröner-Fresenius-Stiftung (2020_EKES.16) (RS).

Competing interests

The authors report no competing interests.

References

1. Lawrence ES, Coshall C, Dundas R, et al. Estimates of the prevalence of acute stroke impairments and disability in a multiethnic population. *Stroke*. 2001;32(6):1279-1284.
2. Koch P, Schulz R, Hummel FC. Structural connectivity analyses in motor recovery research after stroke. *Ann Clin Transl Neurol*. 2016;3(3):233-244. doi:10.1002/acn3.278
3. Rehme AK, Eickhoff SB, Rottschy C, Fink GR, Grefkes C. Activation likelihood estimation meta-analysis of motor-related neural activity after stroke. *Neuroimage*. 2012;59(3):2771-2782. doi:10.1016/j.neuroimage.2011.10.023
4. Grefkes C, Fink GR. Reorganization of cerebral networks after stroke: New insights from neuroimaging with connectivity approaches. *Brain*. 2011;134(Pt 5):1264-1276. doi:10.1093/BRAIN/AWR033
5. Zhu LL, Lindenberg R, Alexander MP, Schlaug G. Lesion load of the corticospinal tract predicts motor impairment in chronic stroke. *Stroke*. 2010;41(5):910-915. doi:10.1161/STROKEAHA.109.577023
6. Schaechter JD, Perdue KL, Wang R. Structural damage to the corticospinal tract correlates with bilateral sensorimotor cortex reorganization in stroke patients. *Neuroimage*. 2008;39(3):1370-1382. doi:10.1016/j.neuroimage.2007.09.071
7. Koch PJ, Rudolf LF, Schramm P, et al. Preserved Corticospinal Tract Revealed by Acute Perfusion Imaging Relates to Better Outcome After Thrombectomy in Stroke. *Stroke*. 2023;54(12):3081-3089. doi:10.1161/STROKEAHA.123.044221
8. Schulz R, Park C-H, Boudrias M-H, Gerloff C, Hummel FC, Ward NS. Assessing the Integrity of Corticospinal Pathways From Primary and Secondary Cortical Motor Areas After Stroke. *Stroke*. 2012;43(8):2248-2251. doi:10.1161/STROKEAHA.112.662619
9. Karbasforoushan H, Cohen-Adad J, Dewald JPA. Brainstem and spinal cord MRI identifies altered sensorimotor pathways post-stroke. *Nat Commun*. 2019;10(1):1-7. doi:10.1038/s41467-019-11244-3
10. Welniarz Q, Dusart I, Roze E. The corticospinal tract: Evolution, development, and human disorders. *Dev Neurobiol*. 2017;77(7):810-829. doi:10.1002/dneu.22455
11. Boccuni L, Meyer S, D'cruz N, et al. Premotor dorsal white matter integrity for the prediction of upper limb motor impairment after stroke. *Sci Rep*. 2019;9(1):19712. doi:10.1038/s41598-019-56334-w
12. Riley JD, Le V, Der-Yeghiaian L, et al. Anatomy of stroke injury predicts gains from therapy. *Stroke*. 2011;42(2):421-426. doi:10.1161/STROKEAHA.110.599340
13. Ito KL, Kim B, Liu J, et al. Corticospinal Tract Lesion Load Originating From Both Ventral Premotor and Primary Motor Cortices Are Associated With Post-stroke Motor Severity. *Neurorehabil Neural Repair*. 2022;36(3):179-182. doi:10.1177/15459683211068441
14. Archer DB, Misra G, Patten C, Coombes SA. Microstructural properties of premotor pathways predict visuomotor performance in chronic stroke. *Hum Brain Mapp*. 2016;37(6):2039-2054. doi:10.1002/hbm.23155
15. Saltao da Silva MA, Baune NA, Belagaje S, et al. Clinical Imaging-Derived Metrics of Corticospinal Tract Structural Integrity Are Associated With Post-stroke Motor Outcomes: A Retrospective Study. *Front Neurol*. 2022;13:804133. doi:10.3389/fneur.2022.804133
16. Ward N. Assessment of cortical reorganisation for hand function after stroke. *J Physiol*. 2011;589(23):5625-5632. doi:10.1113/jphysiol.2011.220939
17. Schulz R, Park E, Lee J, et al. Interactions between the corticospinal tract and premotor-motor pathways for residual motor output after stroke. *Stroke*. 2017;48(10):2805-2811. doi:10.1161/STROKEAHA.117.016834
18. Backhaus W, Braaß H, Higgen FL, Gerloff C, Schulz R. Early parietofrontal network upregulation relates to future persistent deficits after severe stroke—a prospective cohort study. *Brain Commun*. 2021;3(2):1-10. doi:10.1093/braincomms/fcab097
19. Marshall RS, Perera GM, Lazar RM, Krakauer JW, Constantine RC, DeLaPaz RL. Evolution of cortical activation during recovery from corticospinal tract infarction. *Stroke*. 2000;31(3):656-661.
20. Frost SB, Barbay S, Friel KM, Plautz EJ, Nudo RJ. Reorganization of Remote Cortical Regions After Ischemic Brain Injury: A Potential Substrate for Stroke Recovery. *J Neurophysiol*. 2003;89(6):3205-3214. doi:10.1152/jn.01143.2002
21. Quandt F, Bönstrup M, Schulz R, et al. The functional role of beta-oscillations in the supplementary motor area during reaching and grasping after stroke: A question of structural damage to the corticospinal tract. *Hum Brain Mapp*. 2019;40(10):3091-3101. doi:10.1002/HBM.24582
22. Schulz R, Koch P, Zimerman M, et al. Parietofrontal motor pathways and their association with motor function after stroke. *Brain*. 2015;138(7):1949-1960. doi:10.1093/brain/awv100
23. Zholudeva L V., Abraira VE, Satkunendrarajah K, et al. Spinal Interneurons as Gatekeepers to Neuroplasticity after Injury or Disease. *J Neurosci*. 2021;41(5):845-854. doi:10.1523/JNEUROSCI.1654-20.2020
24. Wilson AC, Sweeney LB. Spinal cords: Symphonies of interneurons across species. *Front Neural Circuits*. 2023;17(April). doi:10.3389/fncir.2023.1146449
25. Hubli M, Bolliger M, Limacher E, R. Luft A, Dietz V. Spinal neuronal dysfunction after stroke. *Exp Neurol*. 2012;234(1):153-160. doi:10.1016/j.expneurol.2011.12.025
26. Powell MP, Verma N, Sorensen E, et al. Epidural stimulation of the cervical spinal cord for post-stroke upper-limb paresis. *Nat Med*. 2023;29(3):689-699. doi:10.1038/s41591-022-02202-6
27. Pirondini E, Carranza E, Balaguer J-M, et al. Poststroke arm and hand paresis: should we target the cervical spinal cord? *Trends Neurosci*. 2022;45(8):568-578. doi:10.1016/j.tins.2022.05.002
28. Ganguly K, Khanna P, Morecraft RJ, Lin DJ. Modulation of neural co-firing to enhance network transmission and improve motor function after stroke. *Neuron*. 2022;110(15):2363-2385. doi:10.1016/j.neuron.2022.06.024
29. Campos B, Choi H, DeMarco AT, et al. Rethinking Remapping: Circuit Mechanisms of Recovery after Stroke. *J Neurosci*. 2023;43(45):7489-7500. doi:10.1523/JNEUROSCI.1425-23.2023
30. Kaiser J, Maibach M, Salpeter I, et al. The Spinal Transcriptome after Cortical Stroke: In Search of Molecular Factors Regulating Spontaneous Recovery in the Spinal Cord. *J Neurosci*. 2019;39(24):4714-4726. doi:10.1523/JNEUROSCI.2571-18.2019
31. Jiang Y-Q, Armada K, Martin JH. Neuronal activity and microglial activation support corticospinal tract and proprioceptive afferent sprouting in spinal circuits after a corticospinal system lesion. *Exp Neurol*. 2019;321:113015. doi:10.1016/j.expneurol.2019.113015
32. LaPash Daniels CM, Ayers KL, Finley AM, Culver JP, Goldberg MP. Axon sprouting in adult mouse spinal cord after motor cortex stroke. *Neurosci Lett*. 2009;450(2):191-195. doi:10.1016/j.neulet.2008.11.017
33. Bachmann LC, Lindau NT, Felder P, Schwab ME. Sprouting of Brainstem–Spinal Tracts in

Response to Unilateral Motor Cortex Stroke in Mice. *J Neurosci*. 2014;34(9):3378-3389. doi:10.1523/JNEUROSCI.4384-13.2014

34. Landelle C, Dahlberg LS, Lungu O, Misic B, De Leener B, Doyon J. Altered Spinal Cord Functional Connectivity Associated with Parkinson's Disease Progression. *Mov Disord*. 2023;38(4):636-645. doi:10.1002/mds.29354
35. Weber KA, Chen Y, Wang X, et al. Lateralization of cervical spinal cord activity during an isometric upper extremity motor task with functional magnetic resonance imaging. *Neuroimage*. 2016;125:233-243. doi:10.1016/j.neuroimage.2015.10.014
36. Chu Y, Fricke B, Finsterbusch J. Improving T2*-weighted human cortico-spinal acquisitions with a dedicated algorithm for region-wise shimming. *Neuroimage*. 2023;268(January):119868. doi:10.1016/j.neuroimage.2023.119868
37. Finsterbusch J, Sprenger C, Büchel C. Combined T2*-weighted measurements of the human brain and cervical spinal cord with a dynamic shim update. *Neuroimage*. 2013;79:153-161. doi:10.1016/j.neuroimage.2013.04.021
38. Tinnermann A, Geuter S, Sprenger C, Finsterbusch J, Büchel C. Interactions between brain and spinal cord mediate value effects in nocebo hyperalgesia. *Science (80-)*. 2017;358(6359):105-108. doi:10.1126/science.aan1221
39. Khatibi A, Vahdat S, Lungu O, et al. Brain-spinal cord interaction in long-term motor sequence learning in human: An fMRI study. *Neuroimage*. 2022;253(March):119111. doi:10.1016/j.neuroimage.2022.119111
40. Vahdat S, Lungu O, Cohen-Adad J, Marchand-Pauvert V, Benali H, Doyon J. Simultaneous brain cervical cord fMRI reveals intrinsic spinal cord plasticity during motor sequence learning. *PLoS Biol*. 2015;13(6):1-25. doi:10.1371/journal.pbio.1002186
41. Braaß H, Feldheim J, Chu Y, et al. Association between activity in the ventral premotor cortex and spinal cord activation during force generation — A combined cortico-spinal fMRI study. *Hum Brain Mapp*. 2023;44(18):6471-6483. doi:https://doi.org/10.1002/hbm.26523
42. Giboin LS, Sangari S, Lackmy-Vallée A, Messé A, Pradat-Diehl P, Marchand-Pauvert V. Corticospinal control from M1 and PMv areas on inhibitory cervical propriospinal neurons in humans. *Physiol Rep*. 2017;5(20):e13387. doi:10.14814/phy2.13387
43. Fleischmann R, Triller P, Brandt SA, Schmidt SH. Human Premotor Corticospinal Projections Are Engaged in Motor Preparation at Discrete Time Intervals: A TMS-Induced Virtual Lesion Study. *Front Neuroergonomics*. 2021;2. doi:10.3389/fnrgo.2021.678906
44. Teitti S, Määttä S, Säisänen L, et al. Non-primary motor areas in the human frontal lobe are connected directly to hand muscles. *Neuroimage*. 2008;40(3):1243-1250. doi:10.1016/j.neuroimage.2007.12.065
45. Oldfield RC. The assessment and analysis of handedness: The Edinburgh inventory. *Neuropsychologia*. 1971;9(1):97-113. doi:10.1016/0028-3932(71)90067-4
46. Jenkinson M, Beckmann CF, Behrens TEJ, Woolrich MW, Smith SM. FSL. *Neuroimage*. 2012;62(2):782-790. doi:10.1016/j.neuroimage.2011.09.015
47. Jenkinson M, Bannister P, Brady M, Smith S. Improved Optimization for the Robust and Accurate Linear Registration and Motion Correction of Brain Images. *Neuroimage*. 2002;17(2):825-841. doi:10.1006/nimg.2002.1132
48. De Leener B, Levy S, Dupont SM, et al. SCT: Spinal Cord Toolbox, an open-source software for processing spinal cord MRI data. *Neuroimage*. 2017;145(Pt A):24-43. doi:10.1016/j.neuroimage.2016.10.009
49. Cohen-Adad J, Rossignol S, Hoge R. Slice-by-slice motion correction in spinal cord fMRI: SliceCorr. *Proc 17th Sci Meet Int Soc Magn Reson Med Honolulu*. Published online 2009:3181.
50. De Leener B, Fonov VS, Collins DL, Callot V, Stikov N, Cohen-Adad J. PAM50: Unbiased multimodal template of the brainstem and spinal cord aligned with the ICBM152 space. *Neuroimage*. 2018;165:170-179. doi:10.1016/j.neuroimage.2017.10.041
51. Kasper L, Bollmann S, Diaconescu AO, et al. The PhysIO Toolbox for Modeling Physiological Noise in fMRI Data. *J Neurosci Methods*. 2017;276:56-72. doi:10.1016/j.jneumeth.2016.10.019
52. Glover GH, Li TQ, Ress D. Image-based method for retrospective correction of physiological motion effects in fMRI: RETROICOR. *Magn Reson Med*. 2000;44(1):162-167. doi:10.1002/1522-2594(200007)44:1<162::AID-MRM23>3.0.CO;2-E
53. Chang C, Cunningham JP, Glover GH. Influence of heart rate on the BOLD signal: The cardiac response function. *Neuroimage*. 2009;44(3):857-869. doi:10.1016/j.neuroimage.2008.09.029
54. Birn RM, Diamond JB, Smith MA, Bandettini PA. Separating respiratory-variation-related fluctuations from neuronal-activity-related fluctuations in fMRI. *Neuroimage*. 2006;31(4):1536-1548. doi:10.1016/j.neuroimage.2006.02.048
55. Grefkes C, Eickhoff SB, Nowak D a, Dafotakis M, Fink GR. Dynamic intra- and interhemispheric interactions during unilateral and bilateral hand movements assessed with fMRI and DCM. *Neuroimage*. 2008;41(4):1382-1394. doi:10.1016/j.neuroimage.2008.03.048
56. Woolrich MW, Behrens TEJ, Beckmann CF, Jenkinson M, Smith SM. Multilevel linear modelling for FMRI group analysis using Bayesian inference. *Neuroimage*. 2004;21(4):1732-1747. doi:10.1016/j.neuroimage.2003.12.023
57. Woolrich MW, Ripley BD, Brady M, Smith SM. Temporal autocorrelation in univariate linear modeling of FMRI data. *Neuroimage*. 2001;14(6):1370-1386. doi:10.1006/nimg.2001.0931
58. Mayka MA, Corcos DM, Leurgans SE, Vaillancourt DE. Three-dimensional locations and boundaries of motor and premotor cortices as defined by functional brain imaging: A meta-analysis. *Neuroimage*. 2006;31(4):1453-1474. doi:10.1016/j.neuroimage.2006.02.004
59. Beckmann CF, Jenkinson M, Smith SM. General multilevel linear modeling for group analysis in FMRI. *Neuroimage*. 2003;20(2):1052-1063. doi:10.1016/S1053-8119(03)00435-X
60. RStudio Team. RStudio: Integrated Development Environment for R. Published online 2021. http://www.rstudio.com/
61. Sist B, Fouad K, Winship IR. Plasticity beyond peri-infarct cortex: Spinal up regulation of structural plasticity, neurotrophins, and inflammatory cytokines during recovery from cortical stroke. *Exp Neurol*. 2014;252:47-56. doi:10.1016/j.expneurol.2013.11.019
62. Ueno M, Hayano Y, Nakagawa H, Yamashita T. Intraspinal rewiring of the corticospinal tract requires target-derived brain-derived neurotrophic factor and compensates lost function after brain injury. *Brain*. 2012;135(Pt 4):1253-1267. doi:10.1093/brain/aws053
63. Wiersma AM, Fouad K, Winship IR. Enhancing Spinal Plasticity Amplifies the Benefits of Rehabilitative Training and Improves Recovery from Stroke. *J Neurosci*. 2017;37(45):10983-10997. doi:10.1523/JNEUROSCI.0770-17.2017
64. Crone SA, Quinlan KA, Zagoraiou L, et al. Genetic Ablation of V2a Ipsilateral Interneurons Disrupts Left-Right Locomotor Coordination in Mammalian Spinal Cord. *Neuron*. 2008;60(1):70-83. doi:10.1016/j.neuron.2008.08.009
65. Konsolaki E, Koropouli E, Tsape E, Pothakos K, Zagoraiou L. Genetic Inactivation of Cholinergic C Bouton Output Improves Motor Performance but not Survival in a Mouse Model of Amyotrophic Lateral Sclerosis. *Neuroscience*. 2020;450:71-80. doi:10.1016/j.neuroscience.2020.07.047
66. Zhang J, Lanuza GM, Britz O, et al. V1 and V2b Interneurons Secure the Alternating Flexor-Extensor Motor Activity Mice Require for Limbed Locomotion. *Neuron*. 2014;82(1):138-150. doi:10.1016/j.neuron.2014.02.013
67. Sapir T, Geiman EJ, Wang Z, et al. Pax6 and Engrailed 1 Regulate Two Distinct Aspects of Renshaw Cell Development. *J Neurosci*. 2004;24(5):1255-1264. doi:10.1523/JNEUROSCI.3187-03.2004
68. Alvarez FJ, Jonas PC, Sapir T, et al. Postnatal phenotype and localization of spinal cord V1 derived interneurons. *J Comp Neurol*. 2005;493(2):177-192. doi:10.1002/cne.20711
69. Lukács M, Vécsei L, Beniczky S. Changes in muscle fiber density following a stroke. *Clin Neurophysiol*. 2009;120(8):1539-1542. doi:10.1016/j.clinph.2009.06.001
70. Astrakas LG, Li S, Elbach S, Tzika AA. The Severity of Sensorimotor Tracts Degeneration May Predict Motor Performance in Chronic Stroke Patients, While Brain Structural Network Dysfunction May Not. *Front Neurol*. 2022;13. doi:10.3389/fneur.2022.813763
71. Yu Q, Yin D, Kaiser M, et al. Pathway-Specific Mediation Effect Between Structure, Function, and Motor Impairment After Subcortical Stroke. *Neurology*. 2023;100(6):e616-e626. doi:10.1212/WNL.0000000000201495
72. Potter-Baker KA, Varnerin NM, Cunningham DA, et al. Influence of corticospinal tracts from higher order motor cortices on recruitment curve properties in stroke. *Front Neurosci*. 2016;10(MAR):79. doi:10.3389/fnins.2016.00079
73. He SQ, Dum RP, Strick PL. Topographic organization of corticospinal projections from the frontal lobe: motor areas on the lateral surface of the hemisphere. *J Neurosci*. 1993;13(3):952-980.
74. He SQ, Dum RP, Strick PL. Topographic organization of corticospinal projections from the frontal lobe: motor areas on the medial surface of the hemisphere. *J Neurosci*. 1995;15(5 Pt 1):3284-3306.
75. Morecraft RJ, Ge J, Stilwell-Morecraft KS, Rotella DL, Pizzimenti MA, Darling WG. Terminal organization of the corticospinal projection from the lateral premotor cortex to the cervical enlargement (C5–T1) in rhesus monkey. *J Comp Neurol*. 2019;527(16):2761-2789. doi:10.1002/cne.24706
76. Wise SP. The ventral premotor cortex, corticospinal region C, and the origin of primates. *Cortex*. 2006;42(4):521-524. doi:10.1016/S0010-9452(08)70391-5
77. Usuda N, Sugawara SK, Fukuyama H, Nakazawa K, Amemiya K, Nishimura Y. Quantitative comparison of corticospinal tracts arising from different cortical areas in humans. *Neurosci Res*. 2022;183:30-49. doi:10.1016/j.neures.2022.06.008
78. Braass H, Feldheim J, Chu Y, et al. Association between activity in the ventral premotor cortex and spinal cord activation during force generation-A combined cortico-spinal fMRI study. *Hum Brain Mapp*. Published online 2023. doi:10.1002/hbm.26523
79. Isa T, Kinoshita M, Nishimura Y. Role of direct vs. indirect pathways from the motor cortex to spinal motoneurons in the control of hand dexterity. *Front Neurol*. 2013;4:1-9. doi:10.3389/fneur.2013.00191
80. Niedtfeld I, Kirsch P, Schulze L, Herpertz SC, Bohus M, Schmahl C. Functional connectivity of pain-mediated affect regulation in borderline personality Disorder. *PLoS One*. 2012;7(3):1-9. doi:10.1371/journal.pone.0033293
81. Plow EB, Cunningham DA, Varnerin N, Machado A. Rethinking stimulation of the brain in stroke rehabilitation: Why higher motor areas might be better alternatives for patients with greater impairments. *Neuroscientist*. 2015;21(3):225-240. doi:10.1177/1073858414537381
82. Schulz R, Park E, Lee J, et al. Synergistic but independent: The role of corticospinal and alternate motor fibers for residual motor output after stroke. *Neuroimage Clin*. 2017;15:118-124. doi:10.1016/j.nicl.2017.04.016
83. Paul T, Cieslak M, Hensel L, et al. The role of corticospinal and extrapyramidal pathways in motor impairment after stroke. *Brain Commun*. 2023;5(1):fcac301. doi:10.1093/braincomms/fcac301